

1 **Supplemental material**

2

3 **6-Hydroxypseudooxynicotine dehydrogenase delivers electrons to electron transfer**  
4 **flavoprotein during nicotine degradation by *Agrobacterium tumefaciens* S33\***

5

6

7 Rongshui Wang,<sup>a</sup> Jihong Yi,<sup>a</sup> Jinmeng Shang,<sup>a</sup> Wenjun Yu,<sup>a</sup> Zhifeng Li,<sup>a</sup> Haiyan Huang,<sup>b</sup>  
8 Huijun Xie,<sup>c</sup> Shuning Wang<sup>a#</sup>

9

10 State Key Laboratory of Microbial Technology, Microbial Technology Institute,  
11 Shandong University, Qingdao 266237, People's Republic of China<sup>a</sup>; Institute of Basic  
12 Medicine, Shandong Academy of Medical Science, Jinan 250062, People's Republic of  
13 China<sup>b</sup>; Environment Research Institute, Shandong University, Qingdao 266237, People's  
14 Republic of China<sup>c</sup>

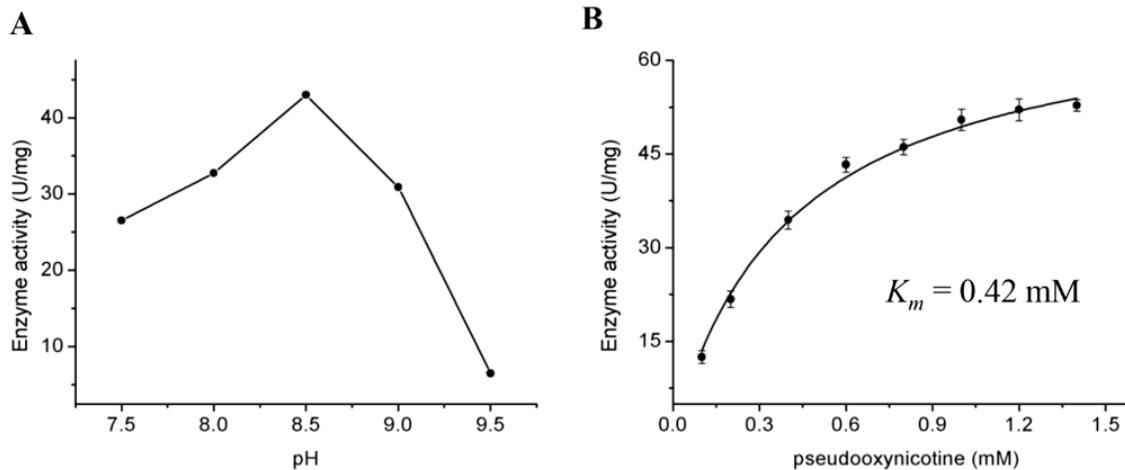
15

16

17 #Address correspondence to Shuning Wang, shuningwang@sdu.edu.cn.

18

19



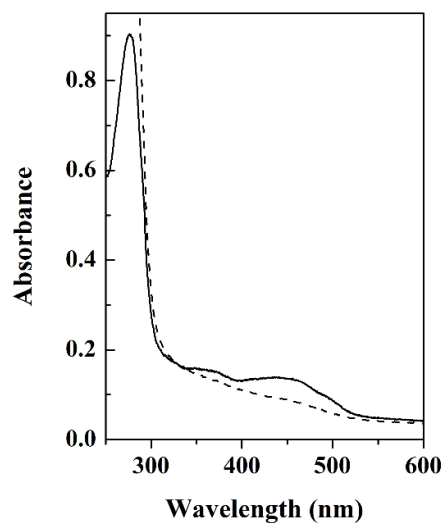
20

21 **FIG S1** Kinetics of pseudooxynicotine dehydrogenation catalyzed by purified Pno with

22 DCPIP (plus PMS) as artificial electron acceptor. (A) Effects of pH on the activity of Pno.

23 (B) Determination of the apparent  $K_m$  of Pno for pseudooxynicotine.

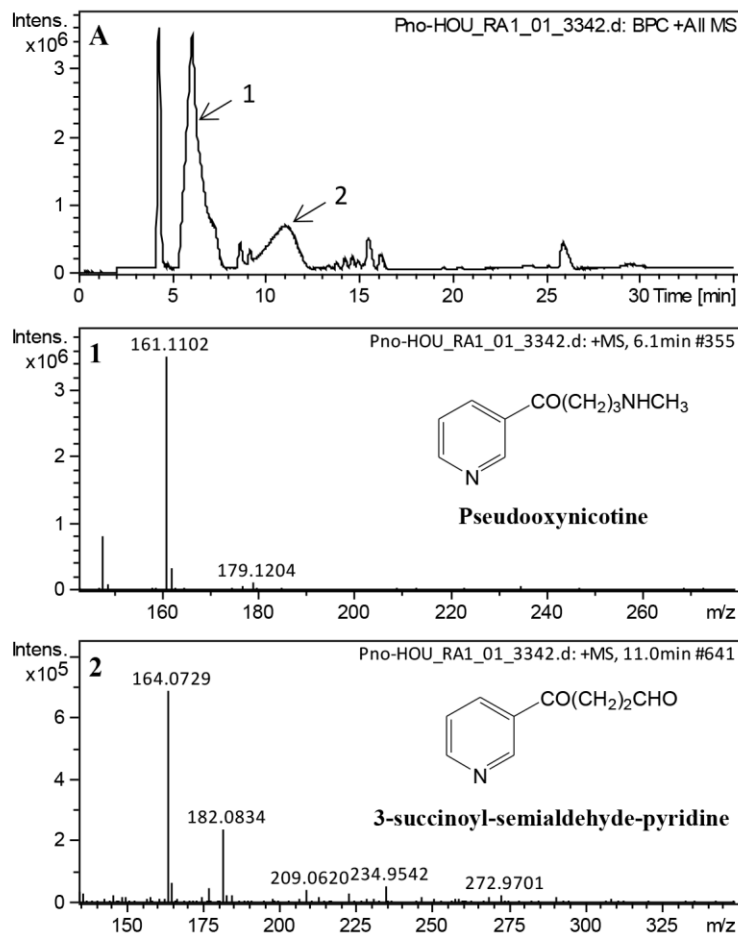
24



25

26 **FIG S2** UV-visible absorption spectra of purified Pno as isolated (solid line) and reduced  
27 by pseudooxynicotine (dashed line). The sample contained 6  $\mu$ M purified protein in 50  
28 mM phosphate buffer (pH 7.0). Pseudooxynicotine was added to 1 mM. The light path of  
29 the cuvette is 3 mm.

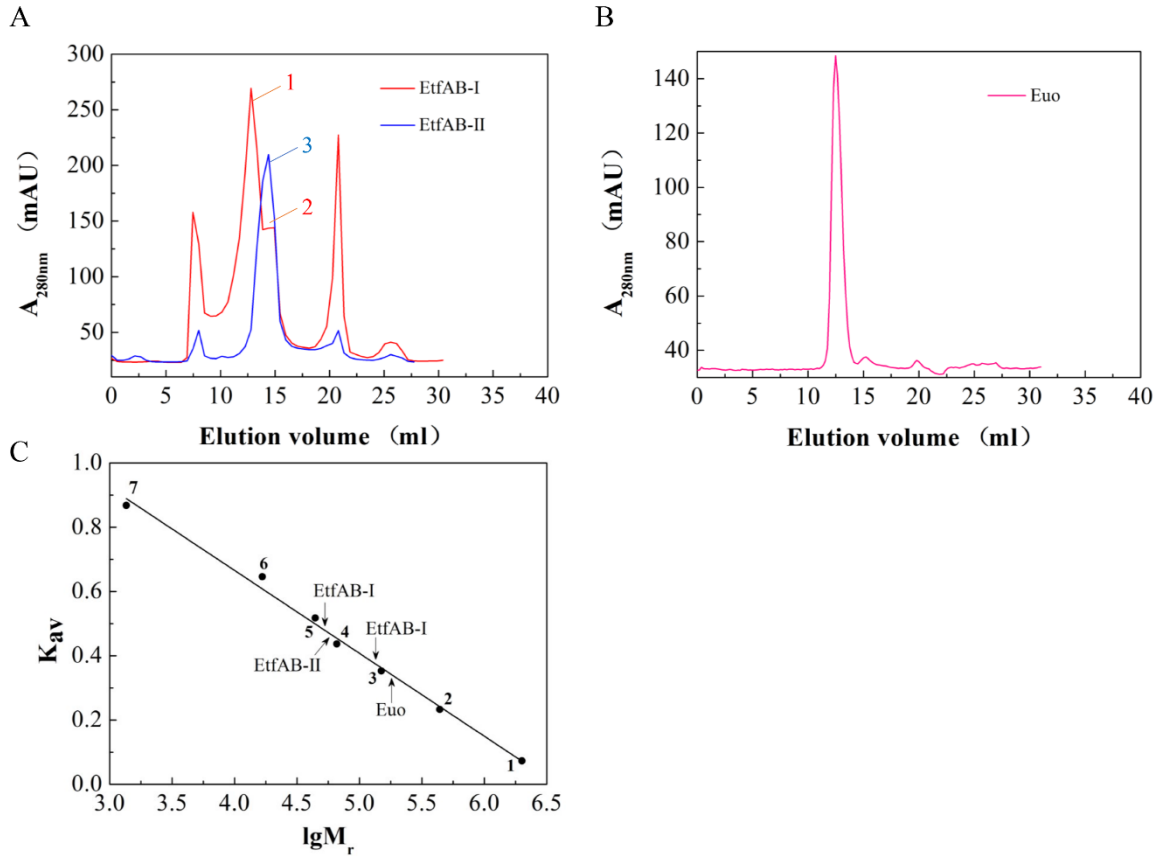
30



31

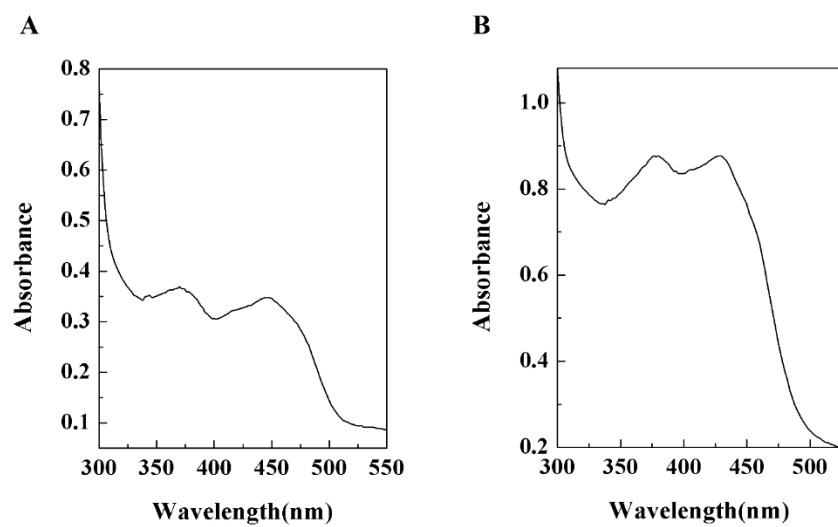
32 **FIG S3** LC-MS profiles of the reaction catalyzed by Pno with pseudooxynicotine as  
 33 substrate. (A) HPLC profile of the products monitoring at 260 nm. (1) Mass spectra of  
 34 the remaining substrate pseudooxynicotine ( $m/z$ , 179.1204) and its dehydrated product  
 35 *N*-methylmyosmine ( $m/z$ , 161.1102). There is a spontaneous hydrolysis equilibrium  
 36 between pseudooxynicotine and *N*-methylmyosmine. (2) Mass spectra of the reaction  
 37 product, 3-succinoyl-semialdehyde-pyridine ( $m/z$ , 164.0729) and its adduct of water ( $m/z$ ,  
 38 182.0834).

39



40

41 FIG S4 Determination of native molecular masses of EtfAB-I (A), EtfAB-II (A), and Euo  
 42 (B) by gel filtration on a GE Superdex G200 column (10 mm×300 mm). The buffer used  
 43 was 50 mM Tris-HCl containing 150 mM NaCl (pH 7.4), and the flow rate was 0.5  
 44 ml min<sup>-1</sup>. (A) peak 1 and peak 2 in red color are EtfAB-I; peak 3 in blue color is EtfAB-II,  
 45 other peaks unlabeled are contaminants. (C) Molecular mass calibration curve. 1, Dextran  
 46 Blue 2000 (2000 kDa); 2, Ferritin from equine spleen (440 kDa); 3,  $\gamma$ -Globulins from  
 47 bovine blood (150 kDa); 4, Bovine serum albumin (66 kDa); 5, Albumin from chicken  
 48 egg white (44.3 kDa); 6, Myoglobin (16.7 kDa); and 7, Vitamin B12 (1,360 Da).



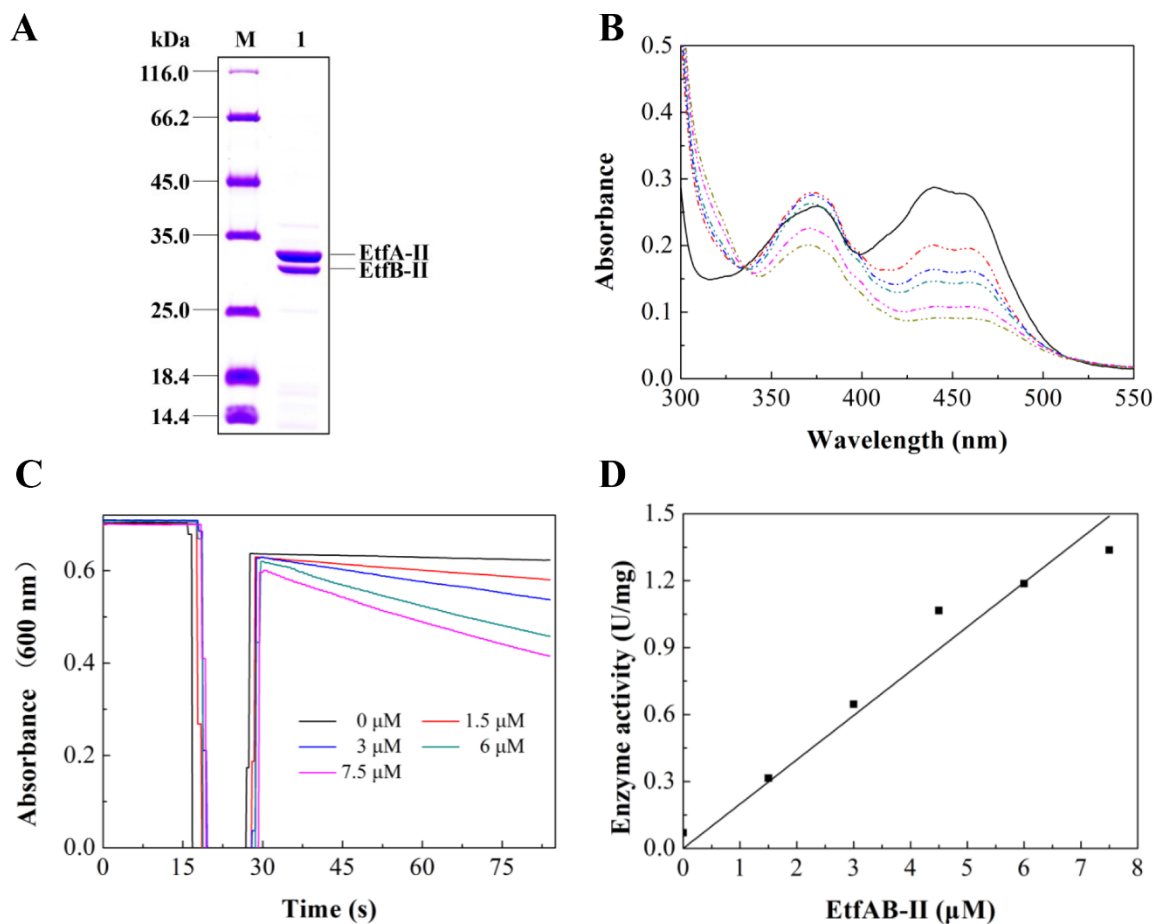
49

50 **FIG S5** UV-visible absorption spectra of purified EtfAB (A) and Euo (B) as isolated. (A)

51 The sample contained 105  $\mu$ M EtfAB-I in 20 mM sodium phosphate buffer (pH 7.4). (B)

52 The sample contained 38  $\mu$ M Euo in 50 mM Tris-HCl (pH 8.5).

53



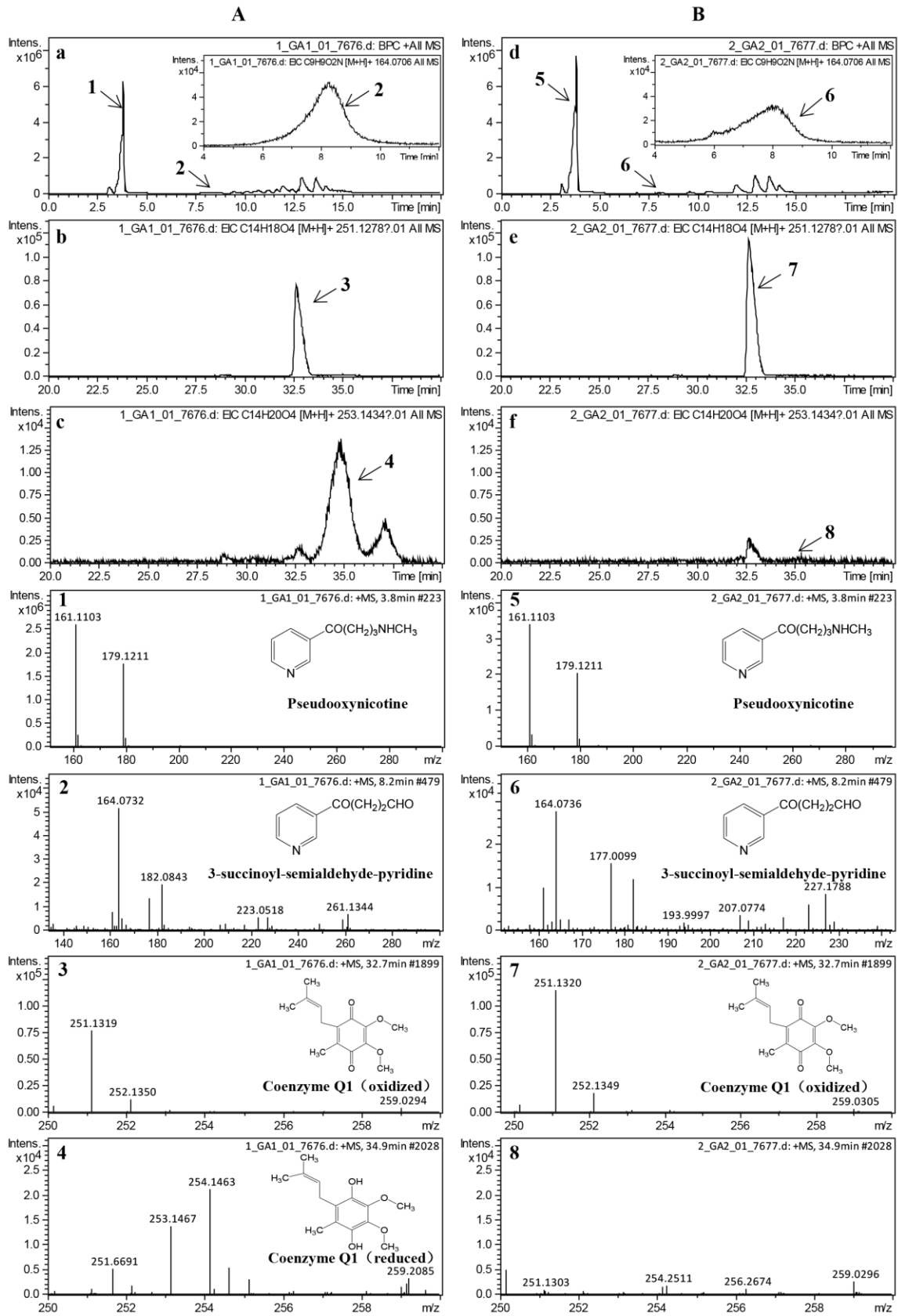
54

55 **FIG S6** Heterologous expression and purification of EtfAB-II and the pseudooxynicotine  
 56 oxidation catalyzed by Pno with purified EtfAB-II as the electron acceptor. (A)  
 57 SDS-PAGE analysis of purified His-tagged EtfAB-II. (B) UV-visible absorption spectra  
 58 of purified EtfAB-II (solid line) and spectrophotometric changes from 300 nm to 550 nm  
 59 during the reduction of EtfAB-II (dash dot dot line) with pseudooxynicotine by Pno.  
 60 Pseudooxynicotine has no absorption in the wavelength window. The reaction mixture  
 61 contained 100 μM EtfAB-II, 1 mM pseudooxynicotine, and 20 mM sodium phosphate  
 62 buffer (pH7.4). The reaction was initiated by adding 0.05 μM of Pno. The red dash dot

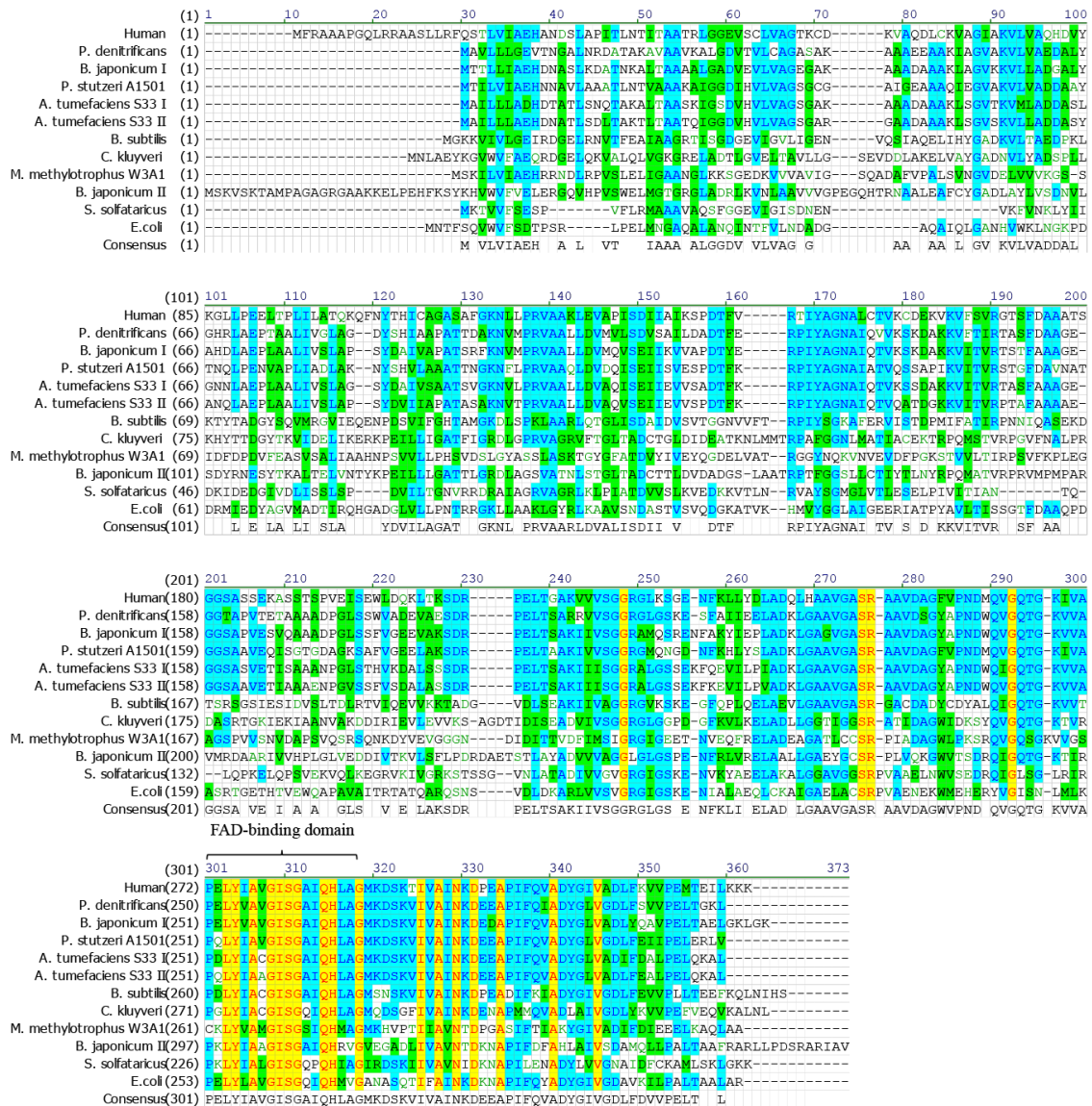
63 dot line is the first record after addition of Pno. Reaction time between the first two  
64 reaction (between black line and red line) was 45 s. The rest records were done every 45 s,  
65 where the absorption continuously decreased. (C) The effect of different concentrations  
66 of EtfAB-II (0-7.5  $\mu$ M) on the reduction of DCPIP by Pno (0.66  $\mu$ M) in the presence of 1  
67 mM pseudooxynicotine monitored at 600 nm. (D) The relationship between the  
68 concentration of EtfAB-II and DCPIP reduction activity (U/mg) catalyzed by Pno. Data  
69 were used from Fig. S6C.

70

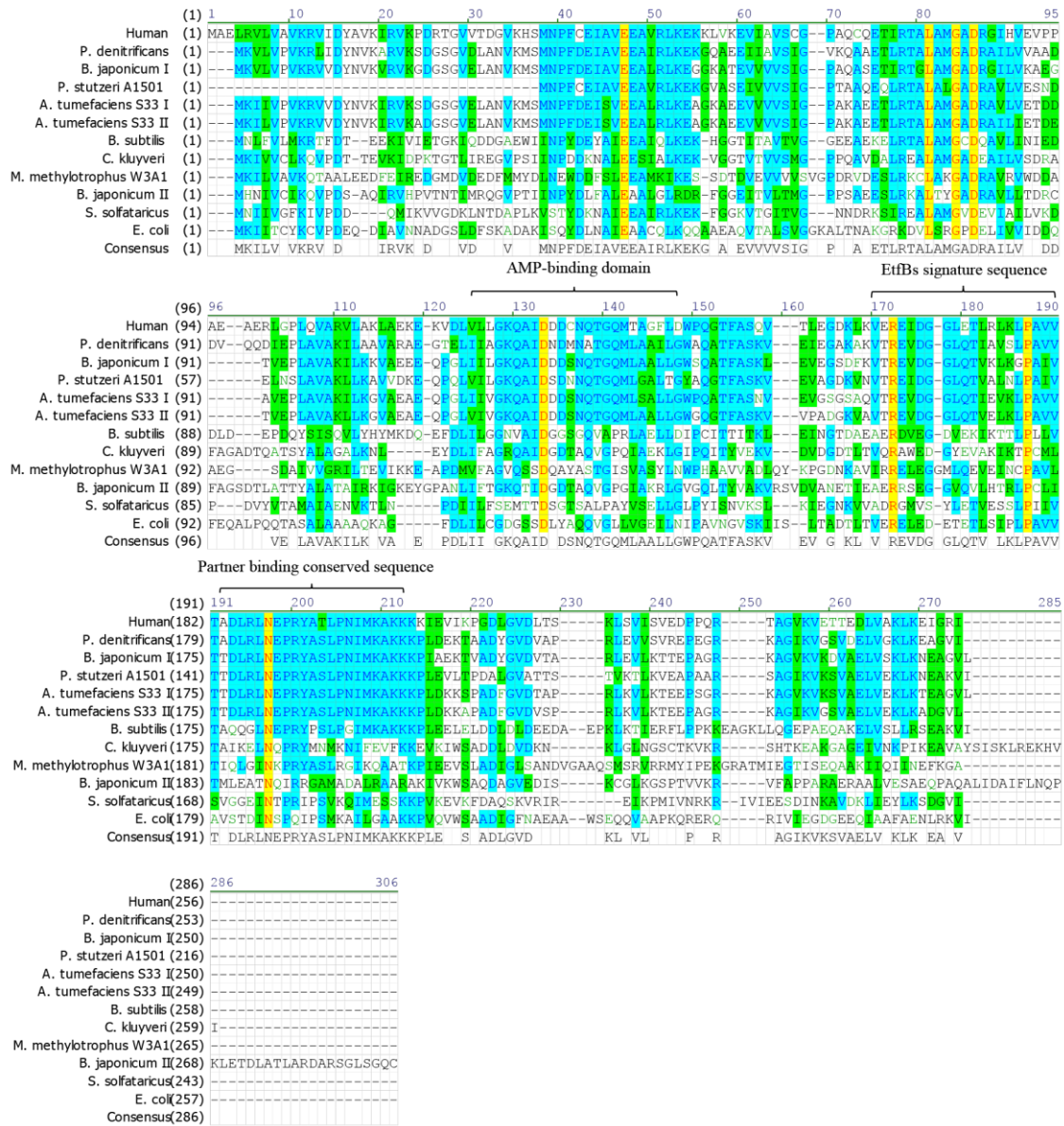




72 **FIG S7** LC-MS profiles of the reaction catalyzed by purified Euo coupling with  
73 pseudooxynicotine oxidation by Pno in the presence of Euo (A) or not (B). The reaction  
74 mixture in 50 mM Tris-HCl (pH 8.5) contained 1 mM pseudooxynicotine, 0.05  $\mu$ M  
75 purified Pno, 8  $\mu$ M purified EtfAB and 32  $\mu$ M CoQ<sub>1</sub>. In (A), 30  $\mu$ M Euo was added.  
76 (a)-(f) Chromatographs of the two samples, where the enlargements of peak 2 and peak 6  
77 are shown in the insets, respectively, in (a) and (d), and the peaks in (b), (c), (e), and (f)  
78 were identified by searching the masses of the expected compounds. (1) and (5) Mass  
79 spectra of the excess substrate pseudooxynicotine ( $m/z$  179.1211) and its spontaneously  
80 dehydrated product *N*-methylmyosmine ( $m/z$  161.1103) with retention time at 3.8 min.  
81 There was a hydrolysis equilibrium between pseudooxynicotine and *N*-methylmyosmine.  
82 (2) and (6) Mass spectra of the product 3-succinoyl-semialdehyde-pyridine ( $m/z$  164.0732  
83 or 164.0736) and its adduct of water ( $m/z$ , 182.0843 or 182.0842) with retention time at  
84 8.2 min. The peaks of ( $m/z$  177.0100 or 177.0099) are possibly caused by the unknown  
85 contaminant in the mobile phase (background signal). (3) and (7) Mass spectra of the  
86 excess oxidized CoQ<sub>1</sub> ( $m/z$  251.1319 or 251.1320) with retention time at 32.7 min. (4)  
87 and (8) Mass spectra of the product reduced CoQ<sub>1</sub> ( $m/z$  253.1467) with retention time at  
88 34.9 min.  
89



92 B EtfBs



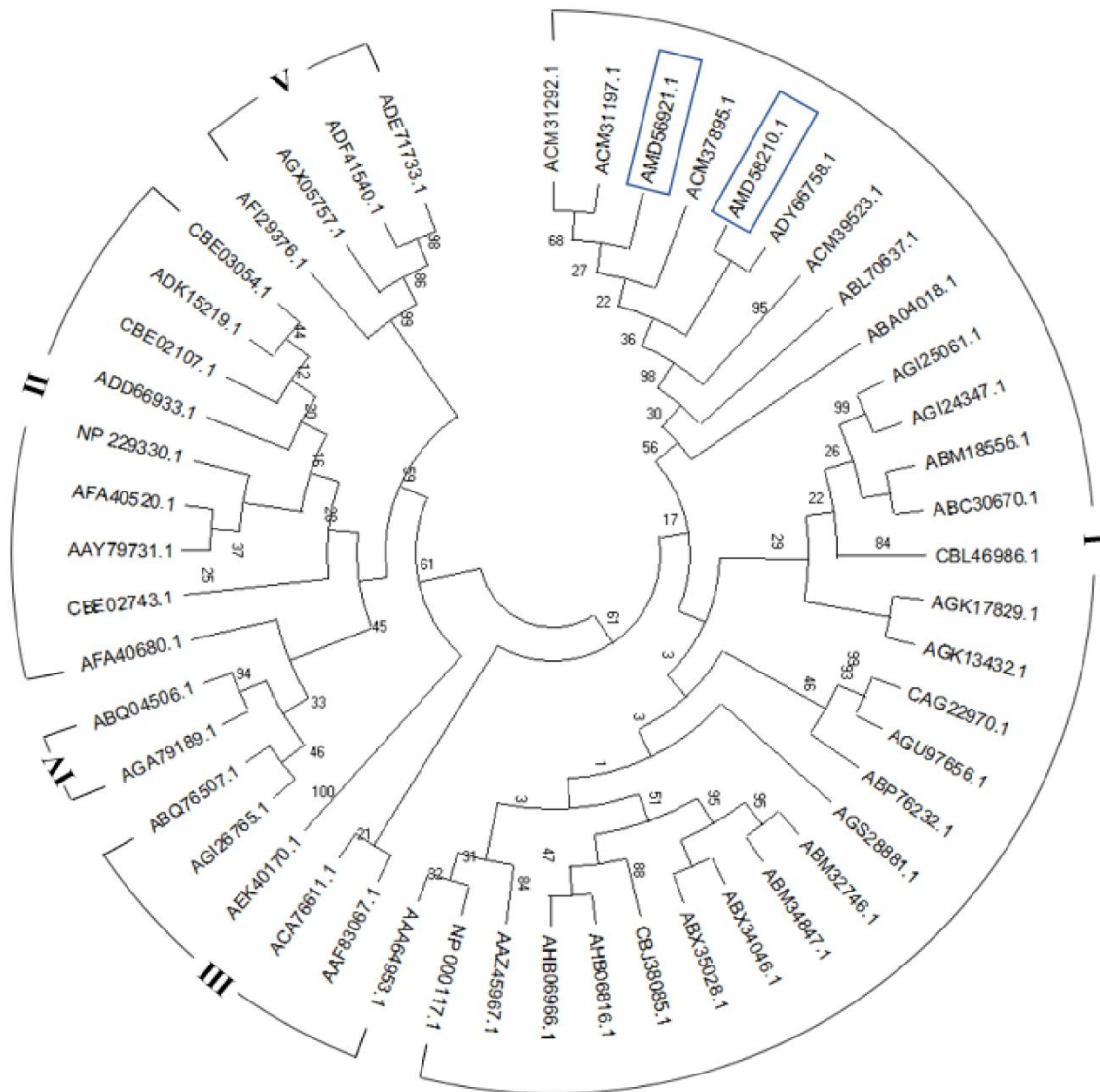
93

94 **FIG S8** Protein sequences alignment of EtfAs (A) and EtfBs (B) from different  
 95 organisms. GenBank/NCBI accession numbers: Human (NP\_000117.1/NP\_001976.1),  
 96 *Paracoccus denitrificans* (ABL70638.1/ABL70637.1), *Bradyrhizobium japonicum* I  
 97 (NP\_768018.1/NP\_768017.1), *Bradyrhizobium japonicum* II

98 (NP\_768413.1/NP\_768678.1), *Pseudomonas stutzeri* A1501 (ABP80254.1/ABP80255.1),  
99 *Agrobacterium tumefaciens* S33 I (AMD56921.1/AMD58724.1), *Agrobacterium*  
100 *tumefaciens* S33 II (AMD58210.1/AMD58211.1), *Methylophilus methylotrophus* W3A1  
101 (AAA64953.1/AAA64952.1), *Sulfolobus solfataricus* (AAK42873.1/AAK42874.1),  
102 *Clostridium kluyveri* (EDK32511.1/EDK32510.1), *Escherichia coli*  
103 (NP\_414584.1/NP\_414583.2), *Bacillus subtilis* (NP\_390730.1/NP\_390731.1). The  
104 sequence alignment was performed with Vector NTI 10. The last line refers to the  
105 consensus sequence. Color code: dark blue foreground and light blue background,  
106 conservative residues; black foreground and light green background, block of similar  
107 residues; red foreground and yellow background, identical residues; dark green  
108 foreground and white background, weakly similar residues; black foreground and white  
109 background, non-similar residues. The conserved AMP-binding sites (responding to  
110 V120-D143 of EtfB from Human) only exist in Group I EtfB from human, *P. denitrificans*,  
111 *B. japonicum* I, *P. stutzeri* A1501, and *A. tumefaciens* S33.

112

113



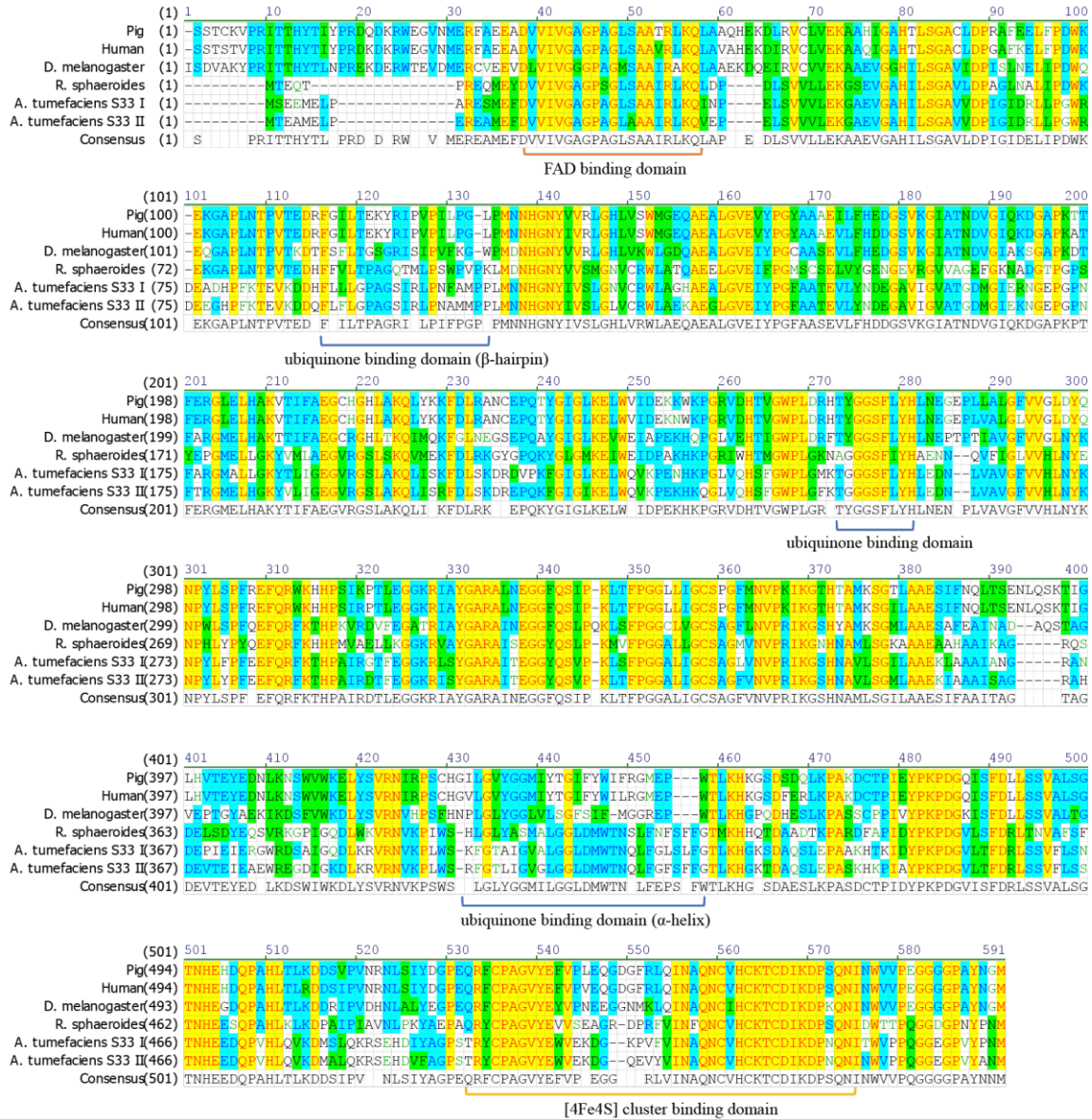
114

115 **FIG S9** Phylogenetic analysis of the EtfABs from different organisms (for details, please  
 116 refer Table S1). The connected protein sequences of EtfA and EtfB were used for analysis.  
 117 Only the GenBank accession numbers of EtfAs are shown. EtfABs from *A. tumefaciens*  
 118 S33 are indicated in blue boxes, where AMD56921.1 is for EtfA-I, and AMD58210.1 is  
 119 for EtfA-II. This tree was inferred by using the Neighbor-Joining method through  
 120 MEGA-X-10.0.5. The evolutionary distances were computed using the JTT matrix-based

121 method and are in the units of the number of amino acid substitutions per site. The rate

122 variation among sites was modeled with a gamma distribution (shape parameter = 1).

123



124

125 **FIG S10** Protein sequences alignment of Euo from different organisms. GenBank  
126 accession numbers: Pig (AAB30031.1), Human (AAN03724.1), *Drosophila*  
127 *melanogaster* (AFH07986.1), *Rhodobacter sphaeroides* (ATN62075.1), *Agrobacterium*  
128 *tumefaciens* S33 I (AMD56919.1), *Agrobacterium tumefaciens* S33 II (AMD61690.1).  
129 Sequences were obtained from NCBI (<https://www.ncbi.nlm.nih.gov/>) with GenBank



130 accession numbers. The mitochondrial targeting sequences of eukaryotic sequences were  
131 removed as Watmough and Frerman (2010) described. The alignment of the six  
132 sequences was performed with Vector NTI 10.  
133

**Table S1** EtfABs from different organisms used for phylogenetic analysis in FIG S9.

Group	GenBank Accession Numbers <sup>a</sup>	Organisms
1	AAF83067.1	<i>Xylella fastidiosa</i> 9a5c
1	AAW60643.1	<i>Gluconobacter oxydans</i> 621H
1	AAZ45967.1	<i>Dechloromonas aromatica</i> RCB
1	ABA04018.1	<i>Nitrobacter winogradskyi</i> Nb-255
1	ABC30670.1	<i>Hahella chejuensis</i> KCTC 2396
1	ABL70637.1	<i>Paracoccus denitrificans</i> PD1222
1	ABM18556.1	<i>Marinobacter aquaeolei</i> VT8
1	ABM32746.1	<i>Acidovorax avenae citrulli</i> AAC00-1
1	ABM34847.1	<i>Acidovorax avenae citrulli</i> AAC00-1
1	ABM94258.1	<i>Methylibium petroleiphilum</i> PM1
1	ABP76232.1	<i>Shewanella putrefaciens</i> CN-32
1	ABX34046.1	<i>Delftia acidovorans</i> SPH-1
1	ABX35028.1	<i>Delftia acidovorans</i> SPH-1
1	ACM31197.1	<i>Agrobacterium radiobacter</i> K84
1	ACM31292.1	<i>Agrobacterium radiobacter</i> K84
1	ACM37895.1	<i>Agrobacterium vitis</i> bv. III S4
1	ACM39523.1	<i>Agrobacterium vitis</i> bv. III S4
1	ADY66758.1	<i>Agrobacterium</i> sp. H13-3
1	AGI24347.1	<i>Pseudomonas denitrificans</i> ATCC 13867
1	AGI25061.1	<i>Pseudomonas denitrificans</i> ATCC 13867
1	AGK13432.1	<i>Azotobacter vinelandii</i> CA
1	AGK17829.1	<i>Azotobacter vinelandii</i> CA6
1	AGS28881.1	<i>Salmonella enterica</i> sv. Newport USMARC-S3124.1
1	AGU97656.1	<i>Vibrio campbellii</i> ATCC BAA-1116
1	AHB06816.1	<i>Pandoraea pnomenusa</i> 3kgm
1	AHB06966.1	<i>Pandoraea pnomenusa</i> 3kgm
1	CAG22970.1	<i>Photobacterium profundum</i> SS9
1	CBJ38085.1	<i>Ralstonia solanacearum</i> CMR15
1	CBL46986.1	<i>gamma proteobacterium</i> sp. HdN1
1	NP_000117.1	<i>Homo sapiens</i>
4	ABQ04506.1	<i>Flavobacterium johnsoniae</i> UW101, ATCC 17061
4	AGA79189.1	<i>Echinicola vietnamensis</i> KMM 6221, DSM 17526
5	ADE71733.1	<i>Bacillus megaterium</i> QM B1551
5	ADF41540.1	<i>Bacillus megaterium</i> DSM 319
5	AFI29376.1	<i>Bacillus</i> sp. JS
5	AGX05757.1	<i>Bacillus infantis</i> NRRL B-14911

Group	GenBank Accession Numbers	Organisms
2A	CBE02107.1	<i>Clostridioides difficile</i> R20291
2A	CBE02743.1	<i>Clostridioides difficile</i> R20291
2A	CBE03054.1	<i>Clostridioides difficile</i> R20291
2B	AAAY79731.1	<i>Sulfolobus acidocaldarius</i> 98-3, DSM 639
2B	ADK15219.1	<i>Clostridium ljungdahlii</i> PETC, DSM 13528
2C1	AFA40520.1	<i>Pyrobaculum oguniense</i> TE7, DSM 13380
2C1	AFA40680.1	<i>Pyrobaculum oguniense</i> TE7, DSM 13380
2D1	NP 229330.1	<i>Thermotoga maritima</i> MSB8
2E	ADD66931.1	<i>Denitrovibrio acetiphilus</i> N2460, DSM 12809
3A	ABQ76507.1	<i>Pseudomonas putida</i> F1
3A	ACA76611.1	<i>Escherichia coli</i> C ATCC 8739
3A	AGI26765.1	<i>Pseudomonas denitrificans</i> ATCC 13867
3C	AAA64953.1	<i>Methylophilus methylotrophus</i> W3A1
3D	AEK40170.1	<i>Amycolatopsis mediterranei</i> S699, ATCC 13685
1	AMD56921.1	<i>Agrobacterium tumefaciens</i> S33(EtfAB-I)
1	AMD58210.1	<i>Agrobacterium tumefaciens</i> S33(EtfAB-II)

136 <sup>a</sup> Only GenBank accession numbers of EtfAs are listed.